Absolute I* quantum yields for the ICN Ã state by diode laser gain versus absorption spectroscopy

Wayne P. Hess and Stephen R. Leone[a)]

Joint Institute for Laboratory Astrophysics, University of Colorado and National Bureau of Standards, and Department of Chemistry and Biochemistry, University of Colorado, Boulder, Colorado 80309-0440

(Received)

Absolute I* quantum yields have been measured as a function of wavelength for room temperature photodissociation of the ICN Ã state continuum. The yields are obtained by the technique of time-resolved diode laser gain-versus-absorption spectroscopy. Quantum yields are evaluated at seven wavelengths from 248 to 284 nm. The yield at 266 nm is 66.0±2% and it falls off to 53.4±2% and 44.0±4% at 284 and 248 nm, respectively. The latter values are significantly higher than those obtained by previous workers using infrared fluorescence. Estimates of I* quantum yields obtained from analysis of CN photofragment rotational distributions, as discussed by other workers, are in good agreement with the I* yields reported here. The results are considered in conjunction with recent theoretical and experimental work on the CN rotational distributions and with previous I* quantum yield results.

I. INTRODUCTION

Photodissociation dynamics of the ICN $\tilde{A}$ state has been an active area of both theoretical[1-6] and experimental[7-18] study. This is due in part to the tractability of the study of linear triatomics by quantum and semiclassical calculations, the relative accessibility of the UV absorption band in ICN, and the ease with which the CN photofragment is probed by laser-induced fluorescence (LIF). Even though a great deal is known about ICN photodissociation, a complete description of the photophysics is complex and a number of problems remain.[1,7,9] The number and nature of the repulsive potential surfaces, as well as the extent of adiabatic and nonadiabatic dissociation pathways are in question.[7,9] The increasing wealth of detailed product state information is, however, clarifying this complicated dissociation process.[7-12,15,18] Several elegant studies have measured the details of the CN product states.[7-12,15,16,18,19] The CN rotational state data show distinct low and high N" rotational distributions; the low and high N" distributions have been ascribed to the I^* and I channels, respectively.[7-9] The I/I^* branching ratio can be estimated by summing over all rotational lines for both the low N" (I^*) and high N" (I) distributions.[7] Since the branching ratios estimated from the CN rotational distributions disagree with the only reported study of wavelength-resolved branching ratios,[10] new measurements of absolute wavelength-resolved I^* yields would help to clarify the ICN $\tilde{A}$ state dissociation behavior.

In this paper we report wavelength-resolved I^* quantum yields for the ICN $\tilde{A}$ state using time-resolved diode laser gain-versus-absorption spectroscopy.[20,21] A cw InGaAsP diode laser is used to probe the transient absorption between the $^2P_{1/2}$ and $^2P_{3/2}$ atomic iodine states. The direct probe of the two level system and the excellent amplitude stability of the diode laser allow for a sensitive and accurate determination of the absolute yields. Since the current study

is motivated by several recent measurements and theoretical studies,[1,7-9] a summary of this previous work is presented here before describing our results.

It is known that there are at least two electronically distinct channels in the dissociation of the $\tilde{A}$ state continuum (210 to ~350 nm). One corresponds to ground state iodine $I(^2P_{3/2})$ + $CN(X^2\Sigma^+)$ and the other to excited iodine $I^*(^2P_{1/2})$ + $CN(X^2\Sigma^+)$.[7-10] While it is energetically possible to produce the electronically excited $CN(A^2\Pi)$, this electronically excited state is not observed in ICN $\tilde{A}$ state photolysis.[14,19] Photolysis at 266 nm produces a CN vibrational distribution that is largely in v"=0 with less than 2% in v"=1 and v"=2.[7,15,16,19] Photolysis in the long wavelength tail ($\lambda \gtrsim 290$ nm) leads to a larger fractional vibrational excitation.[15,18] Fisher et al. find populations of 10% and 2% for v"=1 and v"=2 respectively at 308 nm.[18] At wavelengths longer than 320 nm, however, vibrational excitation is not observed.[9,18] It should be noted that at longer photodissociation wavelengths, hot band absorption becomes increasingly important[18] and at $\lambda \gtrsim 300$ nm the I^* channel is no longer energetically accessible.[15]

The photofragment angular distributions indicate that at 266 nm the transition moment is predominantly parallel.[9,13] There is disagreement as to whether the transition moment has both a parallel component and a minor perpendicular component or if the transition moment contains only a parallel component which accesses a single excited state. In the latter case non-adiabatic electronic curve crossing processes are invoked to explain the distinct I^* + $CN(^2\Sigma^+)$ and $I(^2P_{3/2})$ + $CN(^2\Sigma^+)$ product channels.[8-10] Correlation diagrams support the hypothesis that a single excited state correlating to I^* + CN is accessed by a pure parallel transition. From symmetry arguments it is impossible to have a parallel transition leading to a linear excited state which correlates directly to $I(^2P_{3/2})$ as a product.[2] A curve crossing is likely then,

since the $I(^2P_{3/2})$ channel has been shown to arise from a primarily parallel transition.[9,13] Unpublished MCD results also suggest that the absorption is due to only one electronic state in the region between 210 and 320 nm.[9] A "mixed" transition is supported by measurements of the anisotropy parameter.[8,13] Averages of the reported values for the I^* and I channels are $\beta_{I^*} \approx 1.5$ and $\beta_I \approx 1.2$.[9,13] All measured β values deviate from the maximum value of 2.0, which would be the case if the transition moment is purely parallel and the dissociation is direct. The decrease in anisotropy cannot be explained by eitner reactant rotation prior to dissociation or angular momentum restrictions, i.e., if the molecule is bending prior to and during the dissociation.[8] Previous wavelength-resolved I^* quantum yield measurements have suggested the existence of at least three states underlying the absorption, assuming that nonadiabatic channels are minor.[10] Our results do not find the same structure as reported in Ref. 10.

Several groups have used the technique of pulsed laser photolysis and LIF detection to study the rotational state distributions of the CN fragment.[9,12,14,15,18] Variations of this basic technique have been used to determine the anisotropy of the A state transition,[8,9] the alignment of the CN fragment,[8] the populations of the CN spin rotation components,[9,16] and the vibrational populations as a function of wavelength.[15,18] The experimental rotational distributions obtained by several groups are in excellent agreement.[7-9,14,15] The non-Boltzmann rotational distribution produced in the 266 nm photolysis of room temperature molecules has been described as a convolution of three temperature components.[7,15] The low, medium, and high N" components fit "temperatures" of approximately 50, 500 and 7000 K respectively. The two lowest N" temperature components have been assigned to the I^* channel and the high N" temperature component to the ground

state I atom channel. It is believed that the high N" distribution is derived from a bent excited state while the low N" distributions correspond to a linear dissociation.[8,9,15] The separate summations of these low and high rotational distributions predict I^*/I yields that are very different from those previously obtained by the infrared fluorescence technique.[10]

II. EXPERIMENTAL

The experimental setup has been described previously.[20,21] The general approach employs a two laser pulse and probe technique which is displayed in Fig. 1. An amplified, frequency-doubled pulsed Nd:YAG laser is used to pump a pulsed dye laser. The tunable visible output of the dye laser is frequency doubled to produce 10-15 mJ/pulse of tunable UV light for the photodissociation. At the 248 nm photolysis wavelength, a KrF excimer laser is used. The UV beam is telescoped down to produce a 2 mm diameter beam that is then directed through a 90 cm long pyrex absorption cell.

A commercially available cw InGaAsP diode laser with a total output power P_o of approximately 6 mW is used as the probe laser. The diode radiates equally from both front and back facets. The diode laser light is collimated by antireflection coated compound lenses (Fig. 2). The light from the front facet is passed through a Brewster's angle linear polarizer and a quarter-wave plate and then directed to the experiment. The linear polarizer quarter-wave plate combination serves to isolate the sensitive diode laser from optical feedback which may be caused by back reflection along the optical train. The optic axis of the quarter-wave plate is oriented at 45° to the electric vector of the linearly polarized diode laser emission; this converts the polarization from linear to circular. Back reflected circularly polarized light must pass again through the quarter-wave plate; this converts the circularly polarized

reflection back into linear polarized light whose E vector is rotated by 90°. Further transmission of the rotated linear polarized reflection is blocked by the linear polarizer. The circularly polarized output is telescoped down to produce a 2 mm diameter probe beam that is crossed at small angle with the counterpropagating photolysis beam inside the absorption cell.

Immediately following photolysis of the gas phase ICN, transient gain or absorption of the cw diode laser by the population of I^* and I atoms is detected with a fast (>60 MHz), room temperature Ge photodiode. The signal is subsequently amplified, digitized, and, when necessary, signal averaged.

Light emitted from the rear facet of the diode is collimated and imaged onto a Littrow configuration grating (Fig. 2). The dispersed back-reflected light is frequency selected by tuning the angle of the grating. When light from the desired longitudinal mode of the diode is back-reflected, that particular mode is greatly enhanced at the expense of the other undesired modes. This frequency selective feedback forces the normally multimode laser into nearly single mode operation (Fig. 3). The increased power at the desired wavelength and concurrent line narrowing[22,23] dramatically improves the sensitivity of the technique.

The diode laser is tuned to the iodine $^2P_{1/2} \leftarrow {}^2P_{3/2}$ transition as follows. Approximately 10% of the diode beam is split off prior to the absorption cell and directed through a high temperature furnace (T = 800-1000°C). The furnace contains IBr which is thermally dissociated to produce I atoms. The laser beam intensity exiting the furnace is monitored by a PbS detector. Coarse tuning is accomplished by varying the temperature and forward current of the diode without using the grating (i.e., the optical path between the grating and diode is blocked). By detecting absorption of the diode beam as a function of diode temperature and current the laser is tuned to the strong F'=3 ← F"=4 iodine hyperfine transition. In previous work[20]

only the multimode output after this coarse tuning was used to perform the experiment. Fine tuning of the diode is achieved by monitoring an actual experimental signal from the Ge diode on an oscilloscope. With the grating feedback, the diode is tuned until the signal is maximized. Minor adjustments of current and temperature are performed in an iterative manner. Once the coarse current and temperature settings are established, the dissociation furnace is not necessary and only the fine tuning step is required.

Solid ICN is purified by sublimation or used directly after evacuation. Commercially available O_2, H_2, and Ar are used without further purification. All gases are handled in a standard vacuum system. Typically static fills of the gas mixtures are used for the measurements. A small number of laser pulses (1-8) are required for one measurement.

III. RESULTS

Details of the laser gain versus absorption technique are given in Refs. 20 and 21. Figure 4 displays a typical transient gain versus absorption signal. The entire signal is obtained on a short ~10 μs time scale. Data are obtained on mixtures of solid ICN (room temperature ICN has a vapor pressure of ≈130 Pa = 1.0±0.05 Torr), O_2, H_2 and Ar. The quencher and buffer gases are mixed in the proportion 1:10:89, respectively. The molecular oxygen and hydrogen components rapidly quench the I^* produced by the photolysis pulse. The Ar buffer gas serves to thermalize the CN radicals and I and I^* atoms translationally. This eliminates Doppler velocity effects and ensures that the I/I^* hyperfine sublevels are statistically populated.[24,25] Following photolysis, a prompt gain is observed (Fig. 4). The O_2 and H_2 then quench all of the I^* atoms produced in the dissociation to yield I atoms quantitatively. The signal at longer times (τ > 20 μs) is proportional to the total number of

I and I* atoms produced in the dissociation. The back extrapolated time zero signal is proportional to the population difference of the I* and I atoms initially produced, with the proper degeneracies factored in.

The I* quantum yields are obtained with the following analysis. The I* quantum yield is defined by

$$\phi_{I^*} = \frac{N(^2P_{1/2})}{N(^2P_{1/2}) + N(^2P_{3/2})} \qquad (1)$$

where $N(^2P_{1/2})$ is the number of J = 1/2 atomic fragments and $N(^2P_{3/2})$ is the number of J = 3/2 atomic fragments. In principle this technique can only determine branching ratios, but when it is known that every photon absorbed leads to dissociation and that CN bond cleavage does not occur, then the quantum yields are absolute. The CN bond ($D^o_{298} \sim 184$ kcal mole^{-1}) cannot be broken with the wavelengths used here. In addition, the bond breakage time in ICN photolysis has been measured to be ~600 fs at the relatively long wavelength of 306 nm.[17] It is safe to assume then that I-CN bond breaking does occur for every photoexcitation event. Only the time zero amplitude and long time amplitude are necessary to extract the quantum yields. As mentioned, the probe laser is tuned to the single hyperfine transition $[^2P_{1/2}(F^*=3) \leftarrow {}^2P_{3/2}(F=4)]$. Thus, the ratio of initial to final amplitude is given by:

$$\frac{S_i}{S_f} = \frac{\sum_{F^*} \frac{2F^*+1}{(2F^*+1)} \sigma_{F^*-F} N(^2P_{1/2}) - \sum_{F} \frac{2F+1}{(2F+1)} \sigma_{F-F^*} N(^2P_{3/2})}{\sum_{F} \frac{2F+1}{(2F+1)} \sigma_{F-F^*}[N(^2P_{1/2}) + N(^2P_{3/2})]} \quad . \qquad (2)$$

The symbols F and F^* refer to the ground and excited state iodine hyperfine sublevels, σ_{F-F^*} and σ_{F^*-F} are the absorption and stimulated emission

cross sections, respectively, for the particular F and F^* sublevels. Using well-known relations for the absorption and stimulated emission cross sections, and including suitable assumptions about lineshape parameters, etc.,[20,21] the final expression for the quantum yield of I^*, ϕ_{I^*}, is derived from Eqs. (1) and (2):

$$\phi_{I^*} = \frac{1}{3}\left[\frac{S_i}{S_f} + 1\right] \quad . \tag{3}$$

The amplitude for S_i is defined as positive for gain and negative for absorption, and S_f is always taken as positive. The limits on S_i/S_f are $-1 \rightarrow 2$.

The quantum yields are obtained from the initial and final signal amplitudes in a single time-resolved measurement. The internal normalization inherent in probing the coupled pair of states in the gain versus absorption technique provides a measurement that is insensitive to several experimental parameters. These include probe laser and atomic linewidths, the exact tuning of the probe laser, the pressure of the photolysis gas, the pressures of the quencher and buffer gases, the powers of the photolysis and probe lasers, and the absorption coefficient of the photolysis molecule.

The experimental improvements discussed earlier, i.e., incorporation of the grating and telescoping the photolysis and probe lasers, have increased sensitivity and greatly reduced experimental difficulties. The troublesome thermal lens effect discussed in a previous paper[20] is negligible here. The thermal lens effect is caused by a distortion of the light path due to heating of the gas by the UV laser energy deposition. The reduction of the magnitude of this effect may be due to the lower photolysis laser power ($\lesssim$10 mJ/pulse), the increased strength of the cyanoiodide bond ($D_0 \sim 75$ kcal mole^{-1}) compared to the typical alkyliodide bond ($D_0 \sim 53$ kcal mole^{-1}), and the reduced absorption

of the photolysis laser by the low pressure ICN sample. All three factors serve to reduce the thermal heating of the sample. The number of pulses averaged to obtain sufficient signal to noise has dropped by a factor of 1000, and in some cases a single laser pulse provides an adequate signal. Typical experimental runs now consist of the average of only four laser pulses. It is also possible that in the previous study[20] the diode laser overlapped with some vibrational states (e.g. in C_3F_7I), which would exacerbate the thermal absorption problem.

One source of noise remaining is due to high frequency (>10 MHz) power fluctuations of the diode laser. These fluctuations increase when the grating is used to force single mode operation and may be due to mode competition caused by mechanical instability between the laser diode and the grating. The grating induced power fluctuation is still a relatively minor source of noise and the amplitude stability is excellent with $\Delta P_0/P_0 \leq 10^{-3}$, where ΔP_0 denotes the peak-to-peak power fluctuation. In the final analysis, the major error is simply that associated with back extrapolation of the signals to get S_i and S_f, which is subject to mundane interferences such as electronic pick up.

The four component gas mixture deserves some mention. Molecular oxygen is an efficient quencher of I^* ($k_2 = 2.5 \times 10^{-11}$ cm^3 molec^{-1} s^{-1}),[26] which occurs via near resonant electronic energy transfer:

$$I^*(^2P_{1/2}) + O_2(X^3\Sigma) \underset{k_r}{\overset{k_f}{\rightleftharpoons}} I(^2P_{3/2}) + O_2(^1\Delta_g) \quad . \qquad (4)$$

The back reaction of this process is even more efficient with the ratio of $k_r/k_f = 2.9$.[27] Due to the long radiative lifetimes of I^* and $O_2(^1\Delta_g)$, τ_r = 0.128 s and 3880 s, respectively,[28] it is possible for this equilibration to occur. If it is assumed that the only removal of I^* is by O_2 quenching and radiative processes, then the equilibrium depicted in the above equation is

rapidly established. If the concentration of O_2 is not in large excess over the I^* concentration then a significant equilibrium concentration of I^* may be present at long times. A baseline equilibrium I^* concentration would cause the measured final amplitude S_f to be too small and the measured quantum yield to be too large. Anomalously large quantum yields discussed previously[20] were measured with low pressures of O_2 as the only quencher. A calculation using the measured O_2 pressure and the estimated I^* concentration indicates that those anomalously high yields were very likely due to this equilibration. The addition of a small amount of hydrogen provides a pathway for disposing of the equilibrated electronic energy:

$$I^* + H_2 \rightarrow H_2(v=2) + I \qquad (5)$$

$$H_2(v=2) + H_2(v=0) \rightarrow 2H_2(v=1) \quad . \qquad (6)$$

The nature of the probe technique used here to extract quantum yields requires a collisional environment. Unfortunately, UV photolysis often leads to translationally hot radical production. Thus, chemical reactions of translationally hot radicals could affect the measurement. For example

$$ICN + h\nu \rightarrow I^*(I) + \underline{CN} \qquad (7)$$

$$\underline{CN} + H_2 \rightarrow HCN + H \qquad (8)$$

$$H + ICN \rightarrow HCN + I(I^*) \quad . \qquad (9)$$

Here $\underline{CN}$ indicates a translationally hot CN radical. The above mechanism could produce erroneous results if a high pressure of H_2 is present and step (9) is fast. The inclusion of a large, Ar buffer gas component (P_{Ar} = 6.65 kPa = 50 Torr) serves to thermalize the CN radicals rapidly. Published rate constants[29] indicate that the relevant reactions of thermal CN radicals are slow. In order to check for possible chemical effects the total pressure of

the gas sample, and the ratio of ICN to buffer and quencher gas pressures is varied by a factor of 5. In addition, the photolysis laser power is varied ten fold. No systematic effects are observed, i.e., ϕ_{I^*} varies randomly within $\pm 2\sigma$ of the mean value.

Telescoping of the probe and photolysis lasers increases their power densities approximately three fold. The possibility of multiphoton effects due to high photolysis laser power densities is checked by varying the photolysis laser power as mentioned. The increased power density of the probe laser might also alter the $I(I^*)$ populations by optical pumping. A series of neutral density filters is used to reduce the probe laser power by a factor of 7. The quantum yields are not affected by either of these systematic checks, again ϕ_{I^*} varies randomly within $\pm 2\sigma$ of the mean value. The experimental signal amplitudes however vary linearly with both photolysis and probe laser power as would be expected.

A summary of the quantum yield results is presented along with the previous data and some recent theoretical predictions in Table I. There are both quantitative and qualitative differences between the relative IR fluorescence yields[10] and the yields reported here. Our yields are always greater than the relative fluorescence yields[10] and show a much broader wavelength region of high yield. The fraction of total absorption that leads to I^* is displayed along with our gas phase ICN UV absorption spectrum and several older data in Fig. 5. The sample of ICN for the absorption spectrum is purified by repeated sublimation. The absorption spectrum, which is measured with a commercial spectrometer, is quantitatively different from the only other reported spectrum.[30] The discrepancy is in the central portion of the absorption. The maximum extinction reported here is $\varepsilon(\lambda_{max} = 250\ nm) = 85\ \ell\ mole^{-1}\ cm^{-1}$ versus $\varepsilon(\lambda_{max} = 250\ nm) = 100\ \ell\ mole^{-1}\ cm^{-1}$ reported previously.[30]

Since the relative yields[10] are dependent upon an accurate absorption measurement for both the reference and precursor gases, this could be a source of part of the discrepancy with those earlier measurements (see below).

Another possible source of error in the IR fluorescence yields[10] is the enhancement of 1.3 μm emission due to exciplex formation between the parent iodides and I^*.[31] For example, it was shown that I^* can form the complex[32]:

$$I^* + i\text{-}C_3F_7I \rightarrow i\text{-}C_3F_7I\text{-}I^* \quad . \tag{10}$$

Complexed I^* has a larger emission probability than uncomplexed I^*. At the pressures reported in the fluorescence experiments,[10] however, this effect should account for only a 1% error.[32] The IR fluorescence yields are also scaled relative to the known yield of the standard molecule $i\text{-}C_3F_7I$. In that work, a yield of 0.90, obtained from broadband flash photolysis[33] was used. Recently, we have measured the quantum yield of $i\text{-}C_3F_7I$ at 266 nm and found it to be 1.0.[20] This higher value is in agreement with the results of Smedley and Leone, who also concluded in separate wavelength resolved IR fluorescence measurements that the yield must be essentially 1.0 for $i\text{-}C_3F_7I$.[32] If corrections are made to the IR fluorescence results[10] for the differences in the absorption coefficient and the quantum yield of the standard compound, then the IR fluorescence result at 266 nm agrees very well with the absolute yield reported here; the ϕ_{I^*} values would be 68% (IR) and 66.0% (diode). However, I^* yields at other wavelengths cannot be similarly reconciled. For example, the corrected IR fluorescence[10] yield at 280 nm is 32±4%. If this were the true yield, then the gain-versus-absorption measurement would show not gain but absorption, yet our experiments find a strong gain at 280 nm and a ϕ_{I^*} value of 57.7%. This is the gain-versus-absorption signal that is displayed in Fig. 4.

IV. DISCUSSION

It is well established that the photodissociation of the ICN $\tilde{A}$ state produces I and I^* atoms.[10,11] It is also known that the I^* channel leads to CN rotational distributions which are peaked at low N" and that the I channel produces a CN rotational distribution peaked at high N".[7-9] Nadler et al. have resolved the fractions of individual rotational levels corresponding to the I and I^* channels at 266 nm using sub-Doppler resolution laser-induced fluorescence.[9] The I^* quantum yield is then obtained by summing the appropriate component over all the rotational levels. The yield is found to be approximately 65%, which is in excellent agreement with the value of 66.0% reported here. Product rotational distributions as a function of photolysis wavelength have also been obtained.[7,18] Estimates of the I^* quantum yield may be extracted from these without resolving the rotational Doppler profiles by assuming that the low and high N" distributions correspond to I^* and I products, respectively. The rotational intensities may then be summed to obtain the yield. In this manner the I^* yield at 248 and 280 nm can be estimated to be 35±10% and 61±12%, respectively.[7] These agree well with the values of 44.0±4% and 57.7±2% obtained here. Our I^* yields strongly support this interpretation of the I/I^* channels and their relationship to the rotational distributions.[7-9] The absolute I^* yields also compare favorably with a recent theoretical calculation (Table I).[1]

Except near the peak of the I^* yield at 266 nm, our I^* yields do not agree well with the relative IR fluorescence yields.[10] The disagreement persists even after the relative yields have been rescaled to correct for errors in the reported ICN absorption spectrum[30] and the quantum yield of the C_3F_7I standard compound.

The exact number of excited states involved in the ICN $\tilde{A}$ band photodissociation is a key unresolved issue. Although the maximum number of states involved is not known, there is strong evidence for at least three states being involved. Pitts and Baronavski report[10] that at least three states are evident from the wavelength dependence of the relative I^* quantum yield. Those authors deconvolved the $\tilde{A}$ state absorption by multiplying the I^* quantum yield by the molar extinction coefficient to obtain the absorption due to the I^* state. The remaining absorption was assumed to be due to states correlating with I ground state production. This produces what appears to be three distinct absorptions; however, our results show only two broad features (Fig. 5). There could be a third feature to longer wavelengths, but our measurements have not extended that far. Analysis of the absorptions alone does not address the possibility of nonadiabatic processes. Considering the parallel nature of the transition moment and correlation diagram arguments, which preclude the I atom channel for a linear transition state,[2] the MCD results,[9] and the success of recent theoretical calculations,[1] nonadiabatic processes in the dissociation of ICN also appear to be important.

While three distinct bands are no longer obvious in the $\tilde{A}$ state deconvolution, the results still suggest that at least three states are involved. At 266 nm the parallel component of the transition moment accounts for at least 85% of the absorption.[8,9] The upper state reached by the parallel transition has 0^+ symmetry, is of linear geometry, and correlates with I^* + $CN(^2\Sigma^+)$ products.[2,9] The I^* yield at 266 nm is however, only 66%. Since there are no parallel transitions which correlate to $I(^2P_{3/2})$ + $CN(^2\Sigma^+)$ products for linear ICN,[2,9] there must be a second state which couples non-adiabatically to the linear 0^+ state, perhaps at large internuclear separation (R), in order to account for the $\gtrsim$19% discrepancy. The role of such a nonadiabatic process has

been investigated theoretically.[1] The photodissociation was modeled using classical trajectories. In that work, it was assumed that the direct absorption is exclusively to a linear diabatic excited state which dissociates to form $I^* + CN(^2\Sigma^+, v=0)$. Nonadiabatic transitions to a state of bent geometry, which correlates to $I + CN(^2\Sigma^+, v=0)$, are assumed to occur. The second state must be of bent geometry to be consistent with the high N" rotational distribution found for the $I(^2P_{3/2})$ + CN channel. The calculation attempted to reproduce the I^* quantum yields, the CN rotational distributions and the average rotational energy in each channel, all as a function of photodissociation wavelength.[1] Excellent agreement was found with experimental rotational distributions for 248 and 266 nm photolysis, and good agreement at 280, 290 and 308 nm. At wavelengths longer than 260 nm, the calculated I^* yields agree much better[34] with the absolute yields reported here than with the IR fluorescence yields.[10]

The presence of a third excited state is suggested by the drop in I^* yield for wavelengths shorter than 260 nm. At 248 nm the I^* yield is only 44%. If we assume a Landau-Zener-like velocity dependence for curve crossing then we would expect the I^* yield to monotonically increase as photodissociation wavelength decreases, i.e., less curve crossing to the $I(^2P_{3/2})$ + $CN(^2\Sigma^+)$ channel is expected as velocity through the crossing region increases. It is unlikely that the sharp drop-off in I^* yield from 260 to 248 nm can be accounted for by a single curve crossing at large R. This suggests that a third state, again of bent geometry, is either directly accessed by absorption or is coupled to the linear 0^+ state at short R. The MCD results[9] would suggest the latter. The I^* yield predicted by the two-state theoretical model is an anomalously large 69% at 248 nm. To explain the discrepancy, Goldfield et al.[1] also conclude that a second bent state which couples at short R is involved.

The number of states accessed directly in the $\tilde{A}$ state by absorption is a key unresolved problem and there is much conflicting evidence. There are two alternative but contradictory explanations of the absorption. One explanation is that the absorption transition moment is entirely parallel, and all absorption is to the linear 0^+ state which correlates to $I^* + CN(^2\Sigma^+)$ products. The production of $I(^2P_{3/2}) + CN(^2\Sigma^+)$ products must then occur through non-adiabatic coupling to bent states. This explanation is fostered by the interpretation of a recent MCD experiment which indicates that only one state is directly accessed in the ICN $\tilde{A}$ band absorption.[9] Further support is provided by Nadler et al.[9] who find that for 266 nm dissociation the β values do not change with N" in a regular manner. If perpendicular and parallel transitions contribute separately to the high N" I channel and the low N" I^* channel, respectively, one would expect the β values for low and high N" to differ. They are found to be equal within experimental error.

The second explanation is that the transition moment is a mixture of both parallel and perpendicular components and that more than one excited state is accessed directly in absorption from the ICN ground electronic state. Evidence for a "mixed state direct absorption" is provided by photofragment angular distributions which find β values significantly less than would be expected for a pure parallel transition.[13] Similarly the imperfect alignment of the CN rotor lead to the conclusion that at 266 nm the transition has both parallel and perpendicular character.[8]

Hall et al.[8] carefully analyzed the rotational alignment of the CN fragment and concluded that the imperfect alignment cannot be due to rotation of the CN molecule prior to dissociation or orbital angular momentum caused by bending of the ICN molecule during the dissociation. They believe that the best explanation for the imperfect alignment is that the absorption transition

moment is a mixture of parallel and perpendicular components. They suggest that near 266 nm the transition moment is only 85% parallel and 15% perpendicular, and that at both longer and shorter wavelengths the transition moment becomes more perpendicular. This indicates that the $\tilde{A}$ state absorption consists of a strong central parallel transition with two weaker perpendicular transitions on either side. This suggests that at least three states are involved in the $\tilde{A}$ band photodissociation. The absolute I^* yields decrease sharply below 260 nm. If we assume that the transition moment is purely parallel and accesses only a single linear 0^+ state, then we must postulate an extremely strong coupling to a second bent state to account for the decreasing I^* yields. This is possible, but it seems much less likely than if there is a component of the transition moment which directly accesses a bent state correlating with $I(^2P_{3/2})$ + $CN(^2\Sigma^+)$ products.

It is interesting to speculate upon the role of excited vibrational levels of the ground electronic state in the dissociation. In a recent theoretical study of the UV photodissociation of HCℓ, the chlorine atom branching ratios, $Cℓ(^2P_{1/2})/Cℓ(^2P_{3/2})$, are calculated as a function of dissociation wavelength.[35] The predicted branching ratios are strongly dependent on the vibrational level of the HCℓ ground electronic state. The 321 cm^{-1} ν_2 bending vibration of ICN may analogously affect the I^* branching ratios. At 300 K 15% and 3% of the ICN molecules are thermally excited with one and two quanta of the ν_2 bending vibration, respectively. Our I^* quantum yields agree well with the I^* yields estimated from rotational populations obtained in static cell experiments.[7] A separate set of CN rotational distributions is reported in the same work for molecular beam cooled ICN precursor molecules. The I^* yield estimated from the rotational distributions of cooled ICN are much lower than the static cell I^* yield estimates. The amount of the change increases with wavelength; the

proportion of hot band excitation involved in the $\tilde{A}$ band absorption would also increase with wavelength. This suggests the possibility that when bent ICN is excited into the $\tilde{A}$ continuum it is much more likely to dissociate into ground state products.

If we assume that the absorption is exclusively via a parallel transition, even for bent ICN, then it may be that the bent molecule, when "transported" to the excited state surface, is more likely to find the "crossing seam" and enter the ground state I atom channel than the linear molecules. It may be that the CN-I angle is "in position" to move onto the bent potential surface. If, on the other hand, we allow for direct absorption to a bent excited state which correlates to $I^2P_{3/2}$ + $CN(^2\Sigma^+)$ products, then it is possible that the bent ICN has better Franck-Condon factors than linear ICN to make this transition. In addition, transitions that are forbidden for linear ICN may be allowed for bent ICN. This could provide for some perpendicular component to become active in the transition moment.

V. CONCLUSION

We report absolute I^* quantum yields for the ICN $\tilde{A}$ state as a function of wavelength. Our results disagree with the previous wavelength-resolved I^* yields[10] but agree well with the interpretation of experimental CN rotational distributions and theoretical calculations. We conclude that at least three states, one linear and two bent are involved in interactions in the ICN $\tilde{A}$ continuum. We cannot conclude whether the absorption transition moment has only a parallel component or has both parallel and perpendicular components.

ACKNOWLEDGMENTS

The authors are grateful for the generous support from the National Aeronautics and Space Administration, the Air Force Weapons Laboratory, and the National Science Foundation, which made this project possible.

REFERENCES

[a]Staff Member, Quantum Physics Division, National Bureau of Standards.

1. E. M. Goldfield, P. L. Houston and G. S. Ezra, J. Chem. Phys. 84, 3120 (1986).
2. M. D. Morse, K. F. Freed and Y. B. Band, J. Chem. Phys. 70, 3620 (1979).
3. K. E. Holdy, L. C. Klotz and K. R. Wilson, J. Chem. Phys. 52, 4588 (1970).
4. J. A. Beswick and J. Jortner, Chem. Phys. 24, 1 (1977).
5. U. Halavee and M. Shapiro, Chem. Phys. 21, 105 (1977).
6. R. W. Heather and J. C. Light, J. Chem. Phys. 78, 5513 (1983).
7. W. J. Marinelli, N. Sivakumar and P. L. Houston, J. Phys. Chem. 88, 6685 (1984).
8. G. E. Hall, N. Sivakumar and P. L. Houston, J. Chem. Phys. 84, 2120 (1986).
9. I. Nadler, D. Mahgerefteh, H. Reisler and C. Wittig, J. Chem. Phys. 82, 3885 (1985). Unpublished MCD results of A. Gedanken cited in this work.
10. W. M. Pitts and A. P. Baronavski, Chem. Phys. Lett. 71, 395 (1980).
11. S. T. Amimoto, J. R. Wiesenfeld and R. H. Young, Chem. Phys. Lett. 65, 402 (1979).
12. F. Shokoohi, S. Hay and C. Wittig, Chem. Phys. Lett. 110, 1 (1984).
13. J. H. Ling and K. R. Wilson, J. Chem. Phys. 63, 101 (1975).
14. A. P. Baronavski and J. R. McDonald, Chem. Phys. Lett. 45, 172 (1977).
15. A. P. Baronavski, Chem. Phys. 66, 217 (1982).
16. H. Joswig, M. A. O'Halloran and R. N. Zare, Faraday Discuss. 82, in press.

17. N. F. Scherer, J. L. Knee, D. D. Smith and A. H. Zewail, J. Phys. Chem. 89, 5141 (1985).

18. W. H. Fisher, T. Carrington, S. V. Filseth, C. M. Sadowski and C. H. Dugan, Chem. Phys. 82, 443 (1983).

19. M. J. Sabety-Dzvonik and R. J. Cody, J. Chem. Phys. 66, 125 (1977).

20. W. P. Hess, S. J. Kohler, H. K. Haugen and S. R. Leone, J. Chem. Phys. 84, 2143 (1986).

21. H. K. Haugen, E. Weitz and S. R. Leone, J. Chem. Phys. 83, 3402 (1985).

22. L. Goldberg, H. L. Taylor, A. Dandridge, J. F. Weller and R. O. Miles, IEEE J. Quant. Electr. QE-18, 555 (1982).

23. M. W. Fleming and A. Mooradian, IEEE J. Quant. Electr. QE-17, 44 (1981).

24. W. Theime and E. Fill, Opt. Commun. 36, 361 (1981).

25. J. Vigue, P. Grangier and A. Aspect, Phys. Rev. A 30, 3317 (1984).

26. D. H. Burde and R. H. McFarlane, J. Chem. Phys. 64, 1850 (1976).

27. K. Watanabe, S. Kashiwabara and R. Fujimoto, J. Appl. Phys. 59, 42 (1985).

28. G. A. Fisk and G. N. Hays, J. Chem. Phys. 77, 4965 (1982).

29. Handbook of Bimolecular and Termolecular Gas Reactions, Vol. I., Ed. J. Alister Kerr, Assist. Ed. Stephen J. Moss (CRC Press, Inc., Boca Raton, Florida, 1981).

30. A. V. Yakoleva, Izvest. Akad. Nauk SSSR Ser. Fiz. 14, 517 (1950).
Note: There have been several reports of ICN absorption spectra in the literature, but all seem to refer back to this original work.

31. E. Gerck, Opt. Commun. 41, 102 (1982).

32. J. E. Smedley and S. R. Leone, J. Chem. Phys. 79, 2687 (1983).

33. T. Donohue and J. R. Wiesenfeld, J. Chem. Phys. 63, 3130 (1975).

34. G. S. Ezra (private communication). The computed yields are compromise values since a reasonable fit to the then available I^* yields (Ref. 10) could be made only at the expense of the precise fit to the rotational distributions. Thus the agreement between these calculations and the absolute yields reported here may be even better.

35. S. C. Givertz and G. G. Balint-Kurti, J. Chem. Soc., Faraday Trans. 2, 82, 1231 (1986).

TABLE I. I^* quantum yields from ICN.

Wavelength (nm)	ϕI^* This work (%)	ϕI^* IR fluorescence[a] (%)	ϕI^* Estimated from CN rot. dists.[b] (%)	ϕI^* Theoretical[c] (%)
290	---	---	44±12	33.9
284	53.4±2	---	---	---
280	57.7±2	32±4	61±12	50
277.5	---	35±9	---	---
276	62.9±2	---	---	---
272	64.5±4	---	---	---
270	---	51±3	---	---
266	66.0±2	68±2 65±5[d] 60[e]	65±10	62.5
262	---	60±2	---	---
260	62.5±3	---	---	---
258	---	45±2	---	---
248	44.0±4	---	35±10	69
246.9	---	19±1	---	---
239.5	---	11±1	---	---

[a] IR fluorescence relative to i-C_3F_7I (Ref. 10). Rescaled to correct for errors in absorption and i-C_3F_7I quantum yield.

[b] Estimated from CN rotational levels from ICN dissociated at 300 K except for 248 nm, in which ICN has been cooled (Ref. 7).

[c] Theoretical calculation using classical trajectories (Ref. 1).

[d] From summation of Doppler resolved CN rotational state distributions (Ref. 9).

[e] From the peak area of time of flight spectrum (Ref. 13).

FIGURE CAPTIONS

Fig. 1. Schematic drawing of the experimental apparatus showing the photolysis cell, high temperature I atom absorption cell, pulsed photolysis laser, cw diode probe laser and the signal processing equipment. Both the photolysis and probe lasers are telescoped down to increase power densities.

Fig. 2. Schematic drawing of the diode laser setup showing the anti-reflection (AR) coated collimating lenses, Littrow configuration grating and the polarizer-quarter wave plate optical isolator.

Fig. 3. The emission spectrum of the diode laser under (a) free running conditions; no optical feedback is employed. The diode laser draws a current of 60 mA at 1.25 V. The output power P_o is approximately 4 mW. (b) Single mode operation; frequency selected feedback from the grating forces the diode laser into nearly single mode operation. P_o is equal to the free running configuration to within 0.1%.

Fig. 4. Transient absorption signal from a multicomponent mixture. The total pressure is ~10 kPa (75 Torr). The sample composition is 0.3% ICN, 1% O_2, 10% H_2 and ~89% Ar. Prompt gain is observed following the 280 nm photolysis pulse. The $I^*(^2P_{1/2})$ atoms are then rapidly quenched by O_2 and H_2. The back extrapolated time zero amplitude (S_i), is proportional to the initial inversion density. The long time asymptotic amplitude (S_f) is proportional to the total I atom density produced by the photolysis pulse. Four 10 mJ laser pulses were averaged to obtain this signal.

Fig. 5. The solid line is our measured ICN absorption spectrum, the crosses (×) are values taken from the absorption measurement of Yakoleva (Ref. 30). The solid circles and squares denote the components of the ICN absorption leading to the production of I^* and I, respectively, using the I^* yields reported here. The dotted (• • • •) and dash-dotted (— • — • —) lines denote the components of the absorption leading to I^* and I production using the rescaled IR fluorescence yields of Ref. 10.

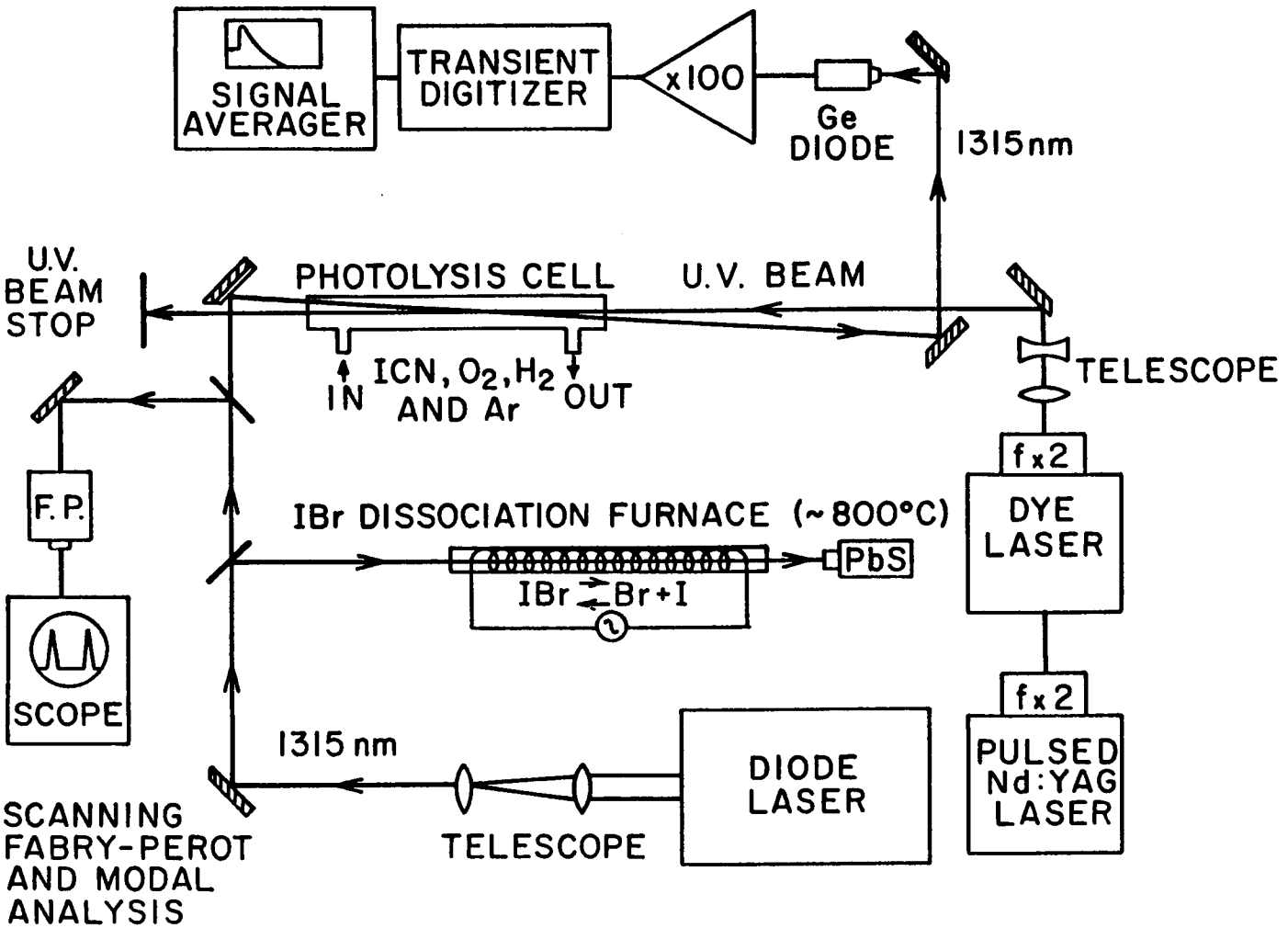
SIGNAL AVERAGER
TRANSIENT DIGITIZER
x100
Ge DIODE
1315nm
U.V. BEAM STOP
PHOTOLYSIS CELL
U.V. BEAM
IN
ICN, O_2, H_2 AND Ar
OUT
TELESCOPE
f x 2
DYE LASER
F.P.
IBr DISSOCIATION FURNACE (~800°C)
PbS
IBr ⇌ Br+I
SCOPE
f x 2
PULSED Nd:YAG LASER
1315 nm
DIODE LASER
SCANNING FABRY-PEROT AND MODAL ANALYSIS
TELESCOPE

Figure 1

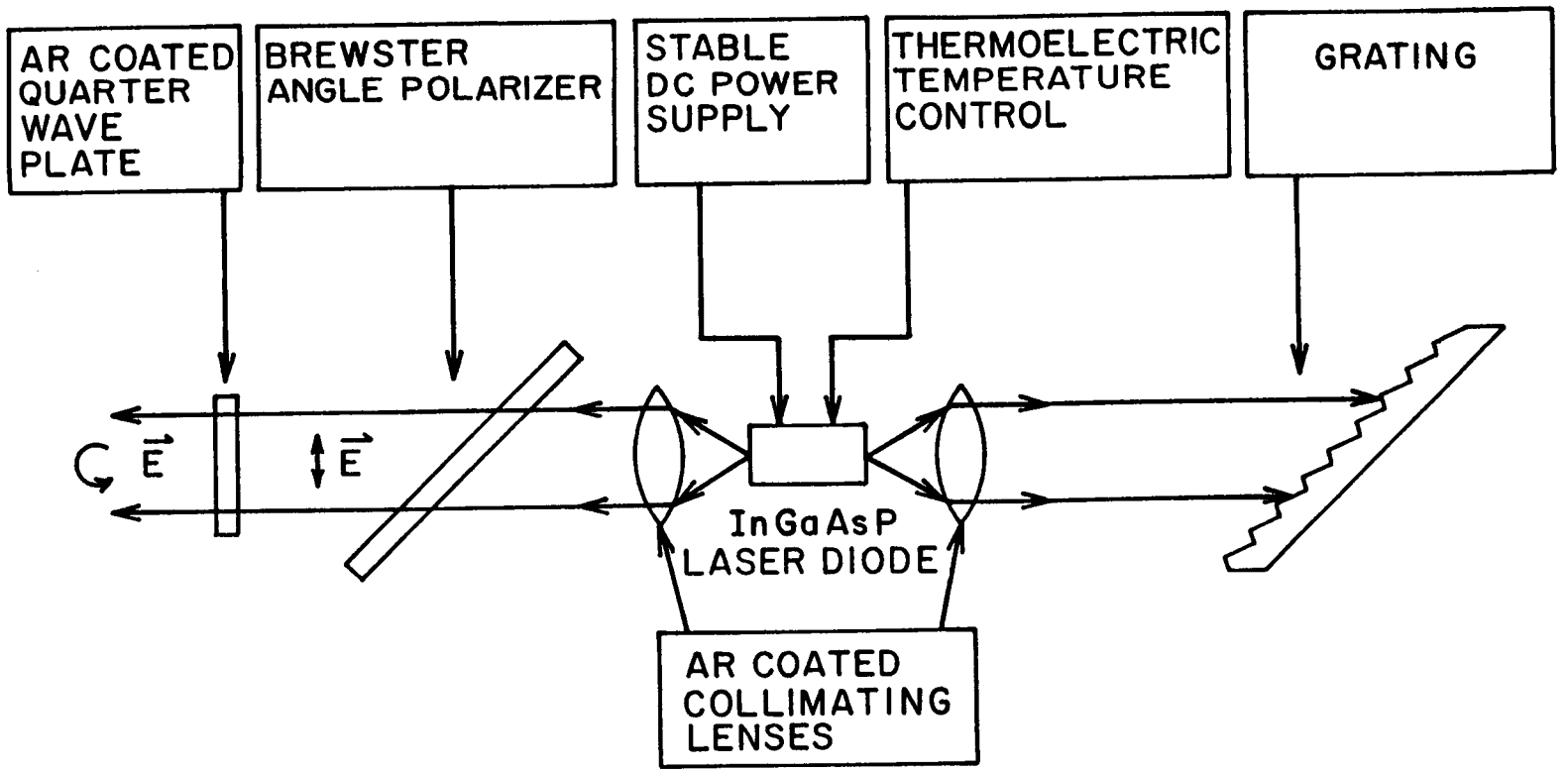
AR COATED QUARTER WAVE PLATE
BREWSTER ANGLE POLARIZER
STABLE DC POWER SUPPLY
THERMOELECTRIC TEMPERATURE CONTROL
GRATING
E
E
InGaAsP LASER DIODE
AR COATED COLLIMATING LENSES

Figure 2

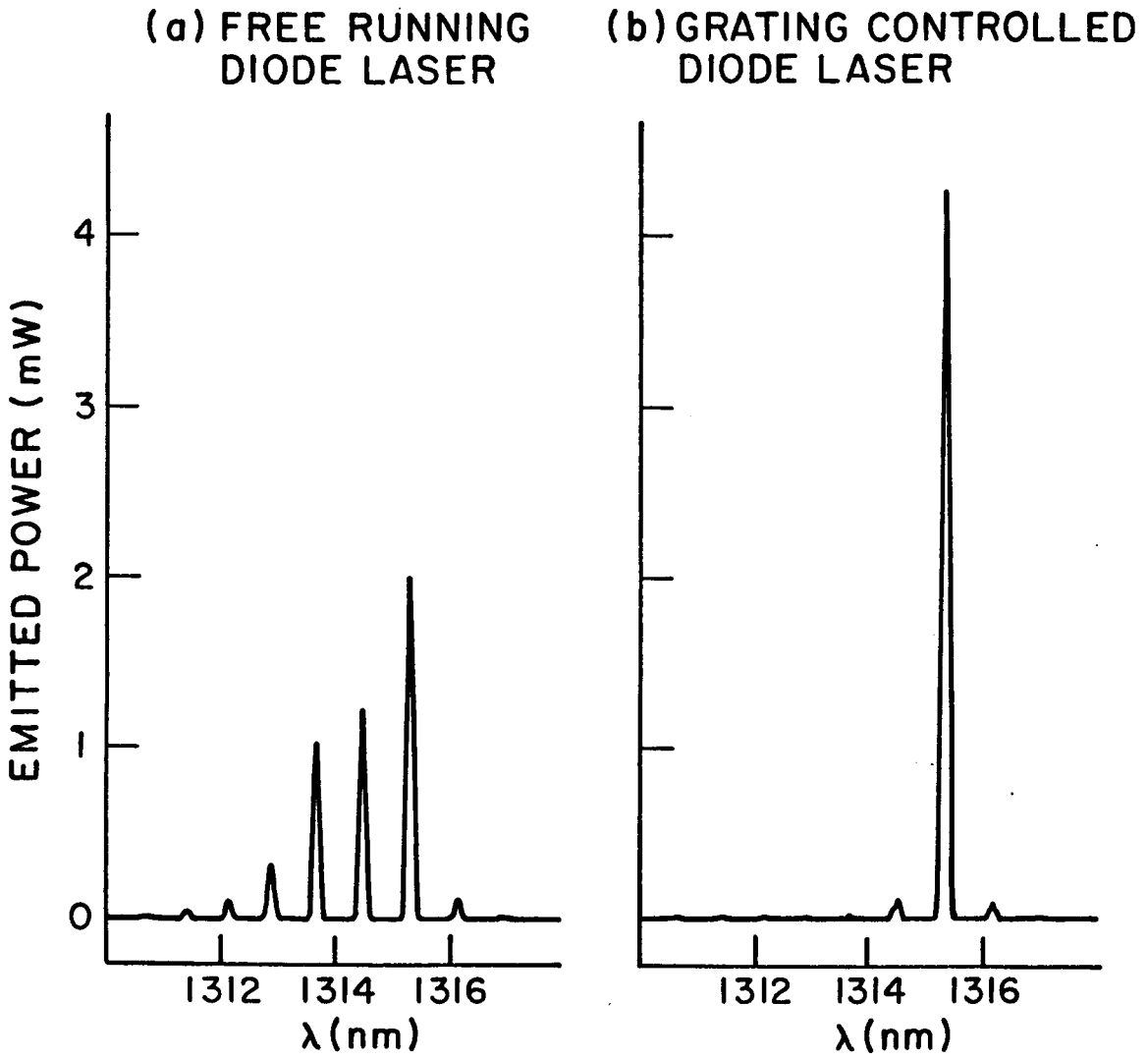
(a) FREE RUNNING DIODE LASER
(b) GRATING CONTROLLED DIODE LASER
EMITTED POWER (mW)
0
1
2
3
4
1312
1314
1316
λ(nm)
1312
1314
1316
λ(nm)

Figure 3

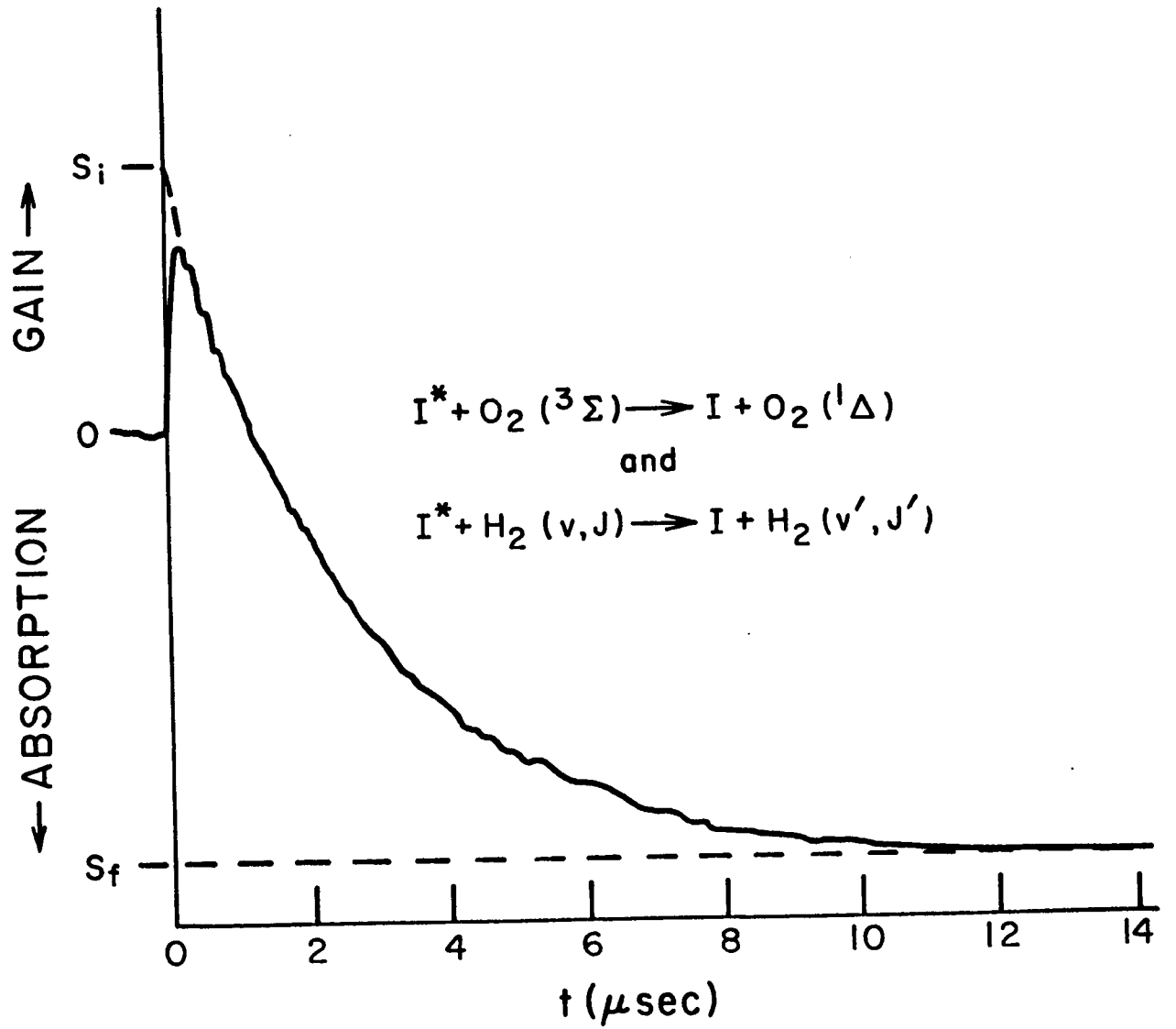
S_i
GAIN →
0
← ABSORPTION
S_f
$I^* + O_2 (^3\Sigma) \rightarrow I + O_2 (^1\Delta)$
and
$I^* + H_2 (v,J) \rightarrow I + H_2 (v',J')$
0
2
4
6
8
10
12
14
t (μsec)

Figure 4

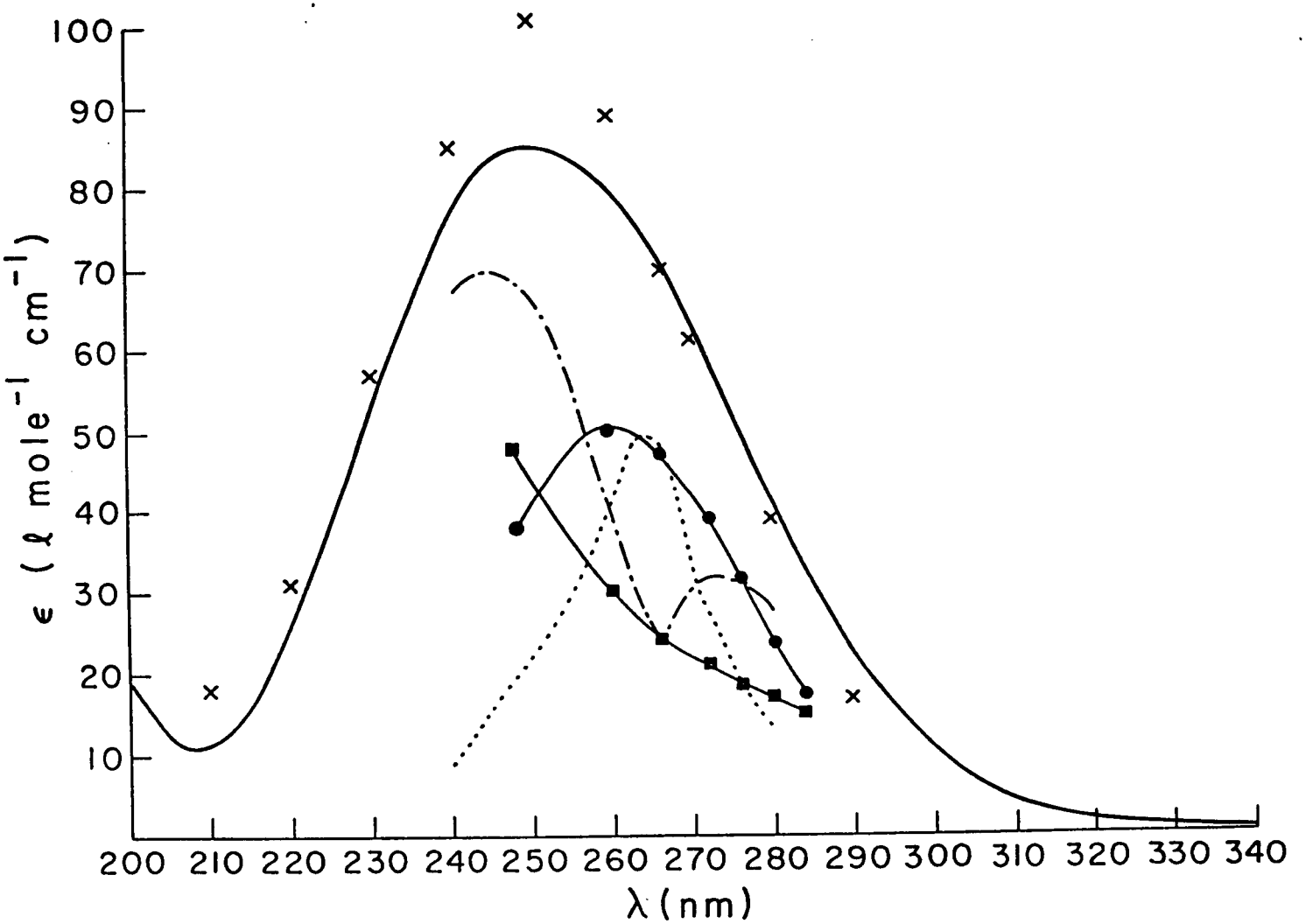
100
90
80
70
60
50
40
30
20
10
ε (ℓ mole⁻¹ cm⁻¹)
200 210 220 230 240 250 260 270 280 290 300 310 320 330 340
λ (nm)

Figure 5